ENTER THE TITLE NAME HERE

A Thesis Submitted to the Faculty

In Partial Fulfillment of the Requirements for the Degree of

Bachelor of Arts

in

Engineering Sciences

by

Abdibaset Ahmed Bare

Thayer School of Engineering
Dartmouth College
Hanover, New Hampshire

June 2025

Advisor: _____

Dr. Kimberly Samkoe
Thayer School of Engineering

Contents

Abstract

This abstract is included in your Thesis. It should contain: Statement of problem, procedure or method, results and conclusions. Max 350 words.

Acknowledgements

I would like to express my sincere gratitude to Dr. Kimberley Samkoe and Dr. Divya Ravi for their invaluable mentorship and steadfast support, which have been instrumental since my freshman summer. As my academic advisor and research mentor, Dr. Samkoe, an Associate Professor at Dartmouth and Principal Investigator of the Samkoe Laboratory, introduced me to the field of research and provided me with the foundational opportunity to join her lab. I am particularly indebted to Dr. Divya Ravi, a recent graduate of the Molecular and Cellular Biology program at the Guarini School of Graduate and Advanced Studies. Her exceptional patience and dedication in training me while she was completing her dissertation were critical to my growth as a research assistant. I also extend my thanks to the entire Samkoe Laboratory, especially Sassan Hodge, Veronica Torres, and Sanjana Pannem, for their collaborative spirit and consistent support with experimental design and data analysis.

This work was generously supported in part by summer internship funding from the E.E. Just Program and a research funding award from the Dartmouth Cancer Center's Student Cancer Research in Immunology Projects (SCRIP).

List of Figures

Chapter 1: Introduction

1.1 Background and Motivation

Programmed cell death protein 1 (PD1) is an immune checkpoint receptor expressed on activated T cells. It functions as an inhibitory receptor, helping to limit excessive immune responses and maintain immune tolerance. PD1 binds to its ligand, programmed death-ligand 1 (PDL1), which is expressed on antigen-presenting cells (APCs) and many other cell types, including both normal and tumor cells. This interaction sends an inhibitory signal to the T cell, reducing its activity and preventing potential collateral tissue damage or autoimmunity. Tumor cells can exploit this mechanism by expressing PDL1, falsely signaling to activated T cells that they are normal cells. This evasion not only facilitates tumor survival but also contributes to T-cell exhaustion and dysfunction [1].

Immune checkpoint inhibitors (ICIs), such as anti-PD1 and anti-PDL1 monoclonal antibodies, block the PD1:PDL1 interaction pharmacologically. Despite their success in improving overall survival in several difficult-to-treat cancers, only a minority of patients experience durable clinical benefits [2]. Clinically, anti-PD1 therapy is often recommended based on tumor PDL1 expression levels [3]. Currently, immunohistochemical (IHC) staining of primary tumors is the standard diagnostic method for assessing PDL1 expression. However, IHC provides only a static snapshot and fails to capture the dynamic nature of PDL1 availability. PDL1 expression is conditional, often transient, and induced by local immune activity, particularly T-cell infiltration.

As a result, IHC may misclassify tumors as PDL1-negative if inflammation is absent at the time of biopsy [4].

Recently, it has been shown that PDL1 can also *cis*-dimerize with CD80 on the same cell surface. This *cis*-interaction reduces the amount of PDL1 available for PD1 binding, potentially impairing the efficacy of therapies targeting this pathway [5]. As a result, surface PDL1 levels alone may not reflect the functional availability of PDL1, complicating its use as a predictive biomarker for ICI response.

Given the limitations of static diagnostic methods like immunohistochemistry, there is a critical need for a dynamic approach to assess the engagement of PDL1 with both PD1 and CD80. The goal of this research is to develop an *in vivo* optical fluorescence imaging technique capable of simultaneously quantifying the expression of PD1, PDL1, and CD80, as well as determining the fraction of PDL1 available for PD1 binding. To accomplish this, we employ a paired-agent imaging (PAI) strategy, which is described in detail below.

1.2 Paired Agent Imaging

PAI is a fluorescence-based molecular imaging technique that involves the simultaneous administration of a receptor-targeted imaging agent and an untargeted control agent, each conjugated to spectrally distinct fluorescent dyes but exhibiting matched pharmacokinetic profiles. By enabling the separation of specific binding from non-specific uptake, PAI's computation model facilitates the quantitative estimation of *in vivo* receptor concentration and availability.

To evaluate immune checkpoint receptor expression, we developed a multi-spectral paired-agent imaging (mPAI) approach capable of simultaneously quantifying the concentrations of PD1, PDL1, and CD80. This methodology involved the co-administration of four monoclonal antibodies: three receptor-targeted antibodies—anti-PD1, anti-PDL1, and anti-CD80 and one untargeted isotype control (IgG). Each antibody was conjugated to a unique fluorophore, enabling multiplexed, spectrally resolved quantification of receptor expression.

Following the quantification of PDL1 expression, a two-agent PAI experiment was conducted

to assess receptor availability. This experiment employed a fluorescently labeled soluble PD1 protein as the targeted agent and a spectrally distinct free dye as the untargeted control. Receptor availability was quantified via calculation of the binding potential, reflecting the accessible fraction of PDL1 capable of engaging PD1.

The PAI experiments utilized near-infrared fluorescent dyes: IRDye680LT (IR680), Alexa Fluor 700 (AF700), Alexa Fluor 750 (AF750), and IRDye800CW (IR800). Imaging was performed using the Pearl® Imaging System, which incorporates two optical detection channels centered at 700 nm and 800 nm. IR680 and AF700 were detected in the 700 nm channel, while AF750 and IR800 were detected in the 800 nm channel, ensuring minimal spectral overlap, and enabling accurate fluorophore discrimination.

1.3 Thesis Structure

This thesis is divided into two main projects. The first is part of a larger project aimed at developing an mPAI framework for simultaneously quantifying multiple immune checkpoint receptors, including PD1, PDL1, and CD80. My contribution focuses specifically on diffusion experiments to determine the diffusion coefficients and times. These diffusion times are critical for establishing appropriate incubation durations in tissue mimicking phantoms inoculated with tumor cells, ensuring reliable agent distribution prior to imaging. A comprehensive account of these diffusion studies, along with the associated experimental protocols, is presented in Chapter 2.

The second project involves a PAI approach using soluble PD1 to quantify the fraction of PDL1 receptors that are functionally available for PD1 binding. A detailed account of this work is provided in Chapter 4. The general structure of the thesis is as follows:

- Chapter 2:Antibody and soluble protein diffusion coefficients - Description of tissue mimicking phantom use for determining diffusion parameters.
- Chapter 3: Selection of fluorophore combinations using liquid phantoms - Identification

of spectrally compatible dyes and assessment of signal interference.

- Chapter 4: PAI: Quantification of functionally available PDL1 for PD1 binding.
- Chapter 5: Future work and global conclusions.

Chapter 2: Antibody and soluble protein diffusion coefficients

2.1 Introduction

To validate the feasibility of both mPAI for quantifying immune checkpoint receptor expression and PAI with soluble PD1 for measuring receptor availability, we first conducted diffusion experiments in tissue mimicking phantoms without cells. These experiments were designed to determine the diffusion coefficients and corresponding diffusion times of fluorescently labeled imaging agents. The results informed the appropriate incubation times needed before imaging experiments in tissue mimicking phantoms with tumor cells.

In biological systems, molecular diffusion arises from the random thermal motion of particles and is a fundamental mechanism governing the transport of substances within tissues. This process is particularly critical in the context of molecular imaging, where the spatial and temporal distribution of imaging agents determines the accuracy of quantitative assessments.

To characterize diffusion behavior *in vitro*, we employed the cell-free, agarose-based tissue mimicking phantoms who protocol is outlined in Section 2.2. Fluorescent images were acquired using the Pearl imaging system, and analyses of the images were performed using MATLAB . A region of interest (ROI) was defined around the central hole where the fluorescent agent was introduced, using an ROI generator implemented in MATLAB. To account for variability in the

shape of the holes in the agar, the ROI was rotated in four angles: $0°, 45°, 90°$, and $135°$. Pixel intensities within the ROI were summed column-wise to generate one-dimensional intensity profiles for each orientation.

To quantify radial diffusion from the hole containing the dye at the center of the well, the full width at half maximum (FWHM) method was applied after subtracting the background signal acquired before dye addition. The diffusion distance at time, t, was thus determined based on the width of the profile at half its maximum intensity, as illustrated in Figure 1.

To determine the diffusion coefficient, we modeled the spread of dye within the agarose phantom as a two-dimensional random walk originating from the hole that contains the dye. The diffusion behavior was quantified using the mean squared displacement (MSD) relation shown in Equation 2.1:

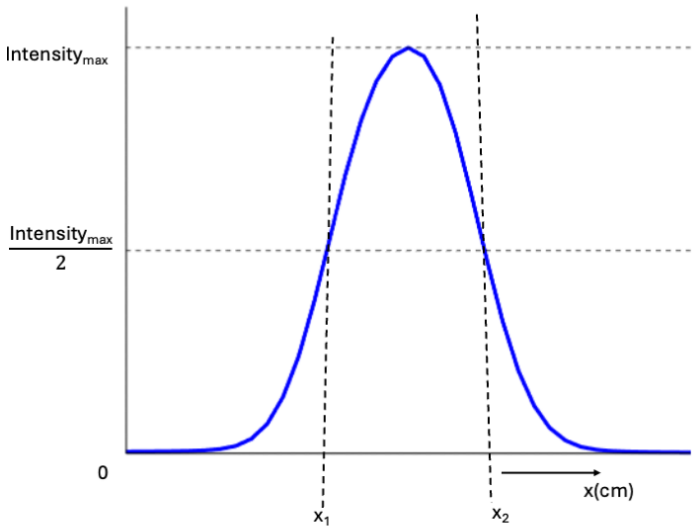

Figure 1. FWHM technique illustration. The curve shows fluorescence intensity as a function of x (cm). FWHM is the width at half-maximum between x_1 and x_2.

$$\langle r^2 \rangle = 4Dt \tag{2.1}$$

where D is the diffusion coefficient (cm^2/s) and t is the time of image acquisition(s).

The experimental time (t_{exp}) required for the fluorescent antibody to distribute evenly throughout the tissue mimicking phantom was determined using Equation 2.1, but using the depth of the tissue mimicking phantom ($x = 0.106cm$) and the experimentally determined

diffusion coefficient (D) above:

$$t_{exp} = \frac{x^2}{4D} = \frac{(0.106cm)^2}{4D} \tag{2.2}$$

Figure 2 presents representative ROI images rotated at four angles ($0°, 45°, 90°$, and $135°$), along with the corresponding intensity peak profiles and $\langle r^2 \rangle$ versus $time$ plots used to calculate diffusion coefficients.

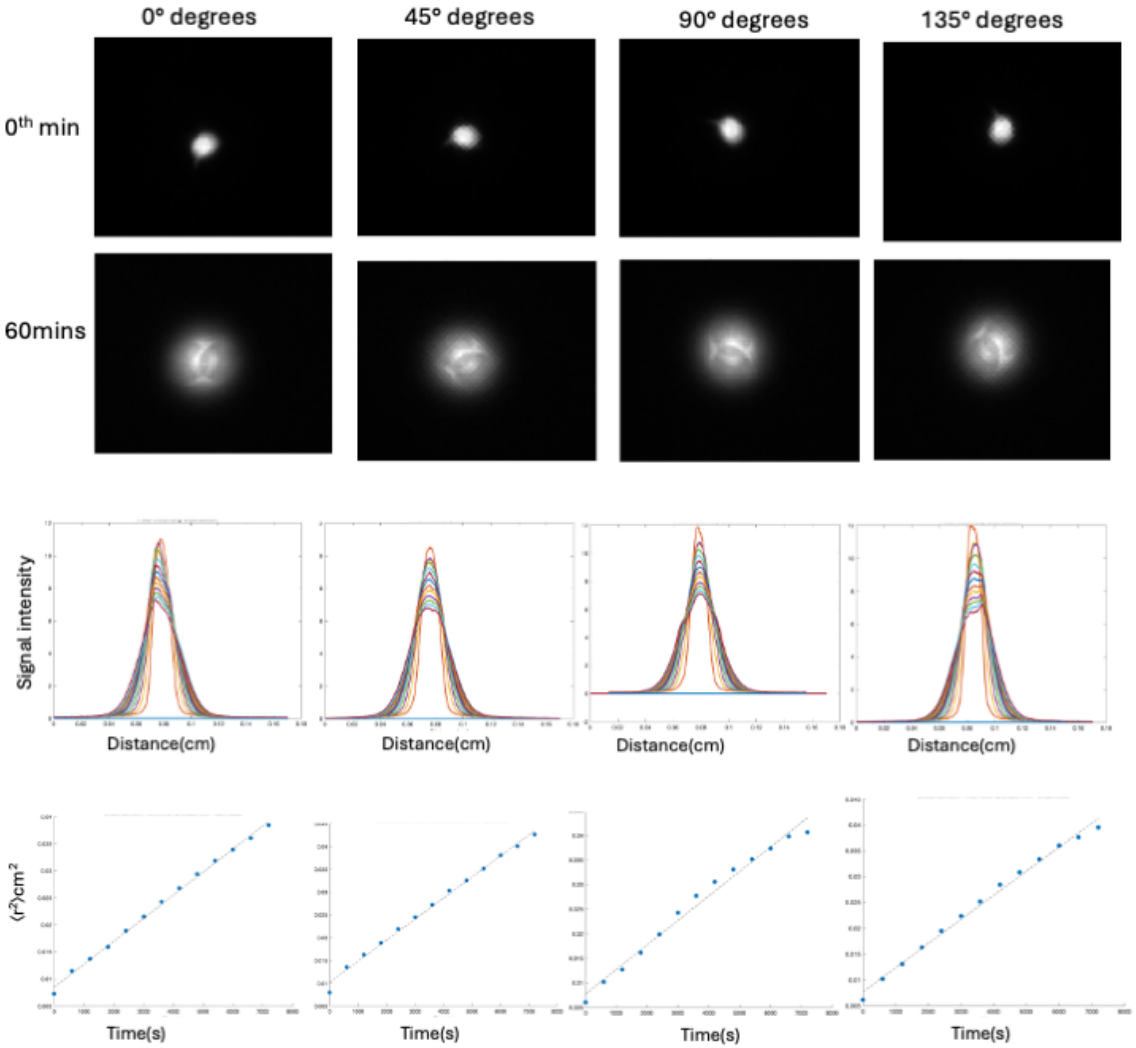

Figure 2. Representative diffusion analysis across four angular directions ($0°, 45°, 90°$, and $135°$). Top panels show fluorescence images of the ROI at 0 and 60 minutes. Middle panels display signal intensity profiles as a function of distance from the center, extracted from each time point and angle. Bottom panels present mean squared displacement, $\langle r^2 \rangle$, versus time plots corresponding to each orientation, used to calculate diffusion coefficients.

For the mPAI experiments, three monoclonal antibodies were used as targeted imaging agents: anti-PD1 was conjugated to IR680, anti-PDL1 to AF750, and anti-CD80 to AF700. An untargeted antibody (IgG) was labeled with IR800. For the PAI experiment involving soluble proteins, a soluble PD1 protein was labeled with IR800 and paired with free IR680 as the untargeted control. These fluorophore-protein pairings were selected based on preliminary liquid phantom experiments (described in Chapter 1) that evaluated fluorescence intensity, linearity, and spectral interference across the Pearl imaging system's detection channels.

2.2 Methods

Agarose based tissue mimicking phantoms protocol

To prepare the tissue phantom, 0.3 g of agarose powder was mixed with 50 mL of phosphate buffered saline (PBS) and heated on a hot plate while stirring until the agarose was fully dissolved, yielding a $0.6\%(w/v)$ agarose solution. The solution was then cooled to approximately $39°C$ before combining 10 mL of the agarose solution with 10 mL of warm PBS to create a $0.3\%(w/v)$ agarose mixture. A volume of 5000 µL of the $0.3\%(w/v)$ agarose mixture was added to each well of a dark-colored, four-well $3D$-printed plate, with each well having a diameter of 35.34 mm and a depth of 19.10 mm. The plate was placed in a digital dry bath and incubated for $15 - 30$ minutes to allow the agarose to solidify. After gelation, a central hole was made in the agarose of each well using a 16-gauge $\times \frac{1}{2}$" Luer stub needle. A background fluorescence image was acquired prior to dye introduction. Then, 12 µL of fluorescent dye was placed into the hole. After dye introduction, fluorescence images were acquired at 5-minute intervals over a 60-minute period. Background images were used for noise subtraction during image analysis.

2.3 Results

As shown in figure 3a, diffusion analysis demonstrated antibodies conjugated to Alexa Fluor-conjugated exhibited significantly higher diffusion coefficients and shorter diffusion

times compared to IRDye-conjugated antibodies.Specifically, anti-CD80 labeled with AF700 and anti-PDL1 labeled with AF750 demonstrated diffusion coefficients of $(9.00 \pm 0.27) \times 10^{-7}\text{cm}^2/\text{s}$ and $(8.35 \pm 0.26) \times 10^{-7}\text{cm}^2/\text{s}$, respectively. In contrast, anti-PD1 labeled with IR680, and the untargeted IgG control labeled with IR800 showed lower diffusion coefficients of $(5.47 \pm 0.48) \times 10^{-7}\text{cm}^2/\text{s}$ and $(4.93 \pm 0.77) \times 10^{-7}\text{cm}^2/\text{s}$, respectively. As a result, the Alexa Fluor-conjugated agents diffused through the 10.6 mm agarose phantom more rapidly, reaching near-equilibrium conditions within 55.3 ± 0.14 minutes for anti-CD80 and 56.6 ± 1.8 minutes for anti-PDL1. In contrast, the IRDye-labeled agents have longer diffusion times with anti-PD1 reaching equilibrium at 86.20 ± 7.8 minutes and the IgG control at 99.7 ± 14 minutes. Based on these results, a standardized incubation period of 120 minutes was adopted for all subsequent mPAI imaging experiments for tissue-mimicking phantoms with cells.

As shown in Figure 3b, the difference between the diffusion coefficients of the free IR680 dye, $(4.93 \pm 0.0017) \times 10^{-6}\text{cm}^2/\text{s}$, and the soluble PD1 conjugated to IR800, $(1.16 \pm 0.0027) \times 10^{-6}\text{cm}^2/\text{s}$, is not statistically significant. Their diffusion times were 34.2 ± 4.0 minutes and 42.2 ± 9.8 minutes respectively. A summary of these data is provided in Table 2.1.

Table 2.1: Summary of mean diffusion coefficients and diffusion times

Imaging Agent	**Mean (standard deviation)**	
	Diffusion Coefficient (cm^2/s)	**Time (mins)**
anti-PDL1-AF750	$(8.35 \pm 0.26) \times 10^{-7}$	56.6 ± 1.8
anti-PD10IR680	$(5.47 \pm 0.48) \times 10^{-7}$	86.2 ± 7.8
anti-CD80-AF700	$(9.00 \pm 0.27) \times 10^{-7}$	55.3 ± 1.4
anti-IgG-IR800	$(4.93 \pm 0.77) \times 10^{-7}$	99.7 ± 14.0
IR800 (free dye)	$(4.93 \pm 0.017) \times 10^{-6}$	34.2 ± 4.0
Soluble PD1-IR800	$(1.16 \pm 0.027) \times 10^{-6}$	42.2 ± 9.8

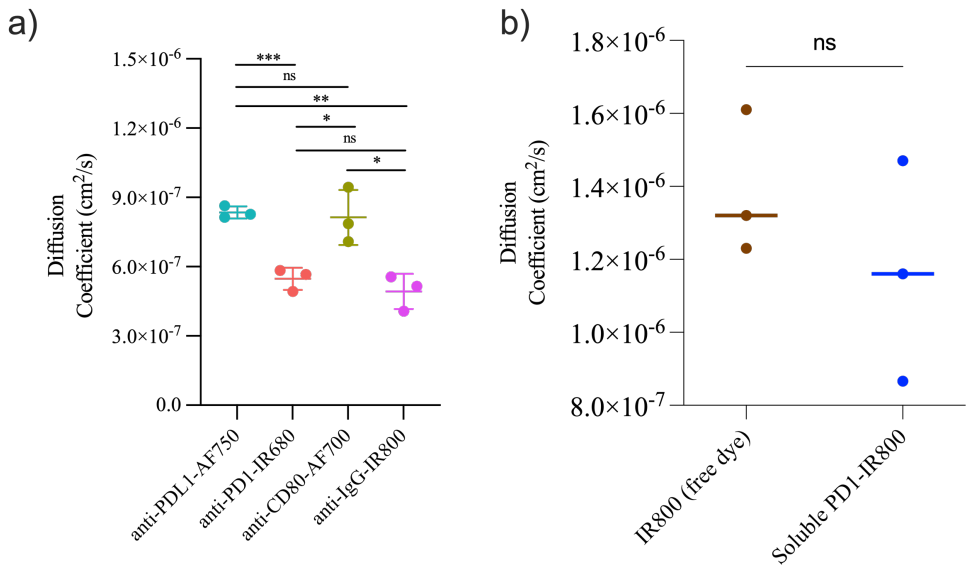

Figure 3. Comparison of the Diffusion Coefficients of Different Imaging Agents. (a) Distribution of diffusion coefficients for antibodies conjugated to fluorophores. Alexa Fluor-conjugated antibodies (PDL1-AF750 and CD80-AF700) exhibited significantly higher diffusion coefficients compared to IRDye-conjugated antibodies (PD1-IR680 and IgG-IR800). (b) Distribution of diffusion coefficients for free IR800 dye and soluble PD1-IR800. Asterisks indicate statistically significant differences, while "ns" denotes non-significant differences.

2.4 Discussion

This study demonstrates the feasibility of using mPAI and PAI with soluble PD1 in tissue mimicking phantoms to quantify immune checkpoint receptor expression and availability. By modeling diffusion as a two-dimensional random walk and applying the mean squared displacement (MSD) relation, we were able to experimentally determine the diffusion coefficients of various fluorescently labeled antibodies, and proteins and calculate the corresponding incubation times required for the imaging to diffuse through the 10.6mm agar layer in prior to imaging experiments with tissue mimicking phantoms with tumor cells.

Our findings show that antibodies labeled with AF750 and AF700 exhibited significantly higher diffusion coefficients than those labeled with IR680 and IR800. This difference suggests that the physicochemical properties of the fluorophores, particularly molecular weight, since

smaller molecules diffuse more rapidly, and hydrophilicity, substantially influence diffusion behavior in the agarose environment. These variations directly affect experimental timing, as faster diffusion results in shorter times to reach equilibrium.

For mPAI, the calculated diffusion times for the various agents ranged from approximately 55 to 100 minutes. For PAI with soluble PD1, these times were shorter, ranging from 34 to 42 minutes. This difference is attributed to the larger molecular weights of antibodies used in mPAI compared to the proteins and free dyes used in PAI with soluble PD1. To ensure sufficient binding and to account for slight variations between agents, we standardized the incubation period: 120 minutes for mPAI and 60 minutes for PAI with soluble PD1. This buffered approach ensures all agents have ample time to reach binding equilibrium before imaging, minimizing the risk of dye wash-off before binding occurs within the tissue mimicking phantoms containing cells.

These findings laid the groundwork for utilizing tissue mimicking phantom with tumor cells to evaluate the binding potential of various imaging agents. Importantly, the ability to capture real-time differences in diffusion and binding supports the broader aim of developing a dynamic platform to quantify PDL1 expression and availability using mPAI and PAI with soluble PD1. This approach advances the potential for imaging-based biomarkers to improve prediction of immune checkpoint inhibitor (ICI) response.

Chapter 3: Selection of fluorophore combinations using liquid phantoms

3.1 Introduction

In the PAI experiment utilizing soluble PD1, it was necessary to identify two fluorescent dyes with spectrally distinct emission profiles suitable for concurrent detection. To guide the selection of appropriate dye pairs, we conducted a series of liquid phantom experiments designed to assess both the linearity of fluorescence signal response and the degree of spectral interference between fluorophores.

Liquid phantoms are optically tunable models designed to mimic the absorption and scattering properties of biological media. In this study, liquid phantoms were employed to evaluate the spectral compatibility of our four fluorescent dyes, ensuring selection of two dyes with minimal signal overlap and enabling accurate quantification of individual receptor concentrations. To validate dye selection, we first conducted linearity tests for each dye individually, followed by combination experiments to assess potential spectral interference. These procedures will be discussed in detail in the subsequent sections.

Linearity tests were performed to determine whether fluorescence signal intensity increased proportionally with dye concentration. This allowed us to identify the linear response range for each fluorophore. Based on these results, we selected a single reference signal intensity that fell within the linear range for all dyes. This signal value was then used to determine the corresponding concentration of each dye in the combination experiments. The liquid phantom

protocols for the linearity and combination studies are presented in Sections 3.2.

3.2 Methods

3.2.1 Liquid phantom protocol for linearity test

To evaluate the linearity of fluorescence signal intensity with respect to dye concentration, we conducted liquid phantom experiments for each fluorescent dye. The dyes were imaged in the detection channels corresponding to their peak excitation wavelengths: IR680 and AF700 in the 700 nm channel, and AF750 and IR800 in the 800 nm channel. IR680 and AF700 were prepared and imaged in a single 96-well plate, as were AF750 and IR800. For each dye, a series of eight concentrations, $0.1nM, 1nM, 10nM, 20nM, 40nM, 60nM, 80nM$, and $100nM$, was prepared. Each concentration was tested in triplicate, resulting in 24 wells per dye to ensure statistical robustness.

Each well contained a total volume of 300 µL, composed of 15 µL of 20% Intralipid, 15 µL of 20% bovine serum albumin (BSA), a calculated volume of dye stock solution, and PBS to complete the volume. The volume of dye stock required to achieve the target final concentration (C_{final}) was determined using the dilution equation 3.1:

$$V_{dye} = \frac{C_{final} \cdot V_{final}}{C_{dye}} \tag{3.1}$$

where V_{dye} is the volume of dye stock solution, C_{final} is the desired final concentration, V_{final} is the total volume of the well, and C_{dye} is the concentration of the dye stock solution. The volume of PBS was adjusted accordingly:

$$V_{PBS} = V_{final} - V_{dye} - V_{Intralipid} - V_{BSA} \tag{3.2}$$

Three replicate wells containing no dye were included on each plate for background subtraction. The image was taken in the Pearl imaging system, and the resulting fluorescence image is analyzed

with ImageJ.

3.2.2 Liquid phantom protocol for combination experiments

Following the determination of the linear response range and the selection of a uniform fluorescence intensity value, we calculated the corresponding dye concentrations that produced this signal within a 300 μL volume. Each dye was then imaged individually and in binary combinations with dyes from the opposite detection channel—for example, IR680 alone and in combination with AF750 and IR800.

As with the linearity experiments, each well was prepared with a total volume of 300 μL, including 15 μL of 20% Intralipid, 15 μL of 20% BSA, the required volume(s) of dye stock solution, and the PBS volume. The individual volumes of each dye were calculated using the same dilution equation 1 described above, and PBS was added to complete the total volume. A schematic of the 96-well plate layout is provided in Figure 4.

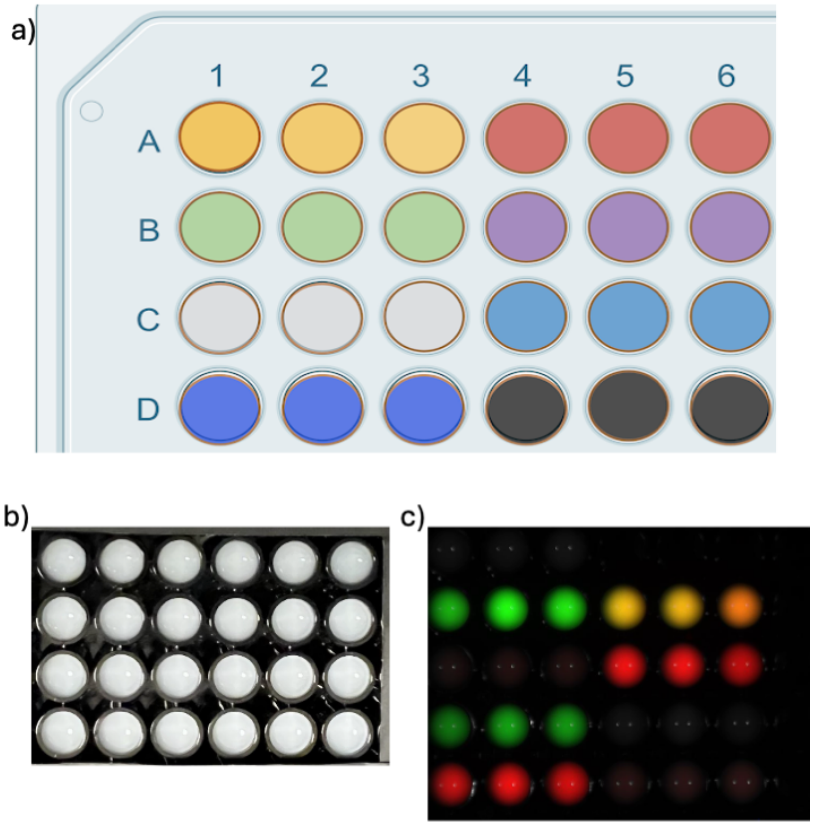

Figure 4. Combination fluorophore experiments set up. (a) Plate map showing the layout of dye combinations and controls in a 96-well plate. Wells A1-A3 contain combinations of AF700 with IR800; A4-A6 contain IR680 with IR800. Wells B1-B3 contain AF700 with AF750; B4-B6 contain IR680 with AF750. Row C contains single-agent controls: IR800 (C1-C3) and AF750 (C4-C6). Row D contains IR680 (D1-D3) and AF700 (D4-D6). Wells E1-E3 are dye-free controls. (b) Image of the 96-well plate prior to imaging. (c) Representative fluorescence image from the Pearl Imaging System showing spectral separation of the fluorophores.

3.3 Results

As shown in Figure 5, all four dyes exhibited a linear correlation between concentration and signal intensity. To enable consistent comparison across agents, a signal intensity value of 0.2, within the linear range for all dyes, was used to determine the corresponding concentrations in the combination liquid phantom experiments. The concentration required to reach this signal varied by dye: AF700 required the lowest concentration ($21.30nM$), followed by AF750 ($46.28nM$),

IR680 ($92.68nM$), and IR800 ($282.00nM$).

In the combination experiments, raw fluorescence intensity measurements were collected for individual dyes and their binary mixtures. These results are summarized in Figures 6 and 7.

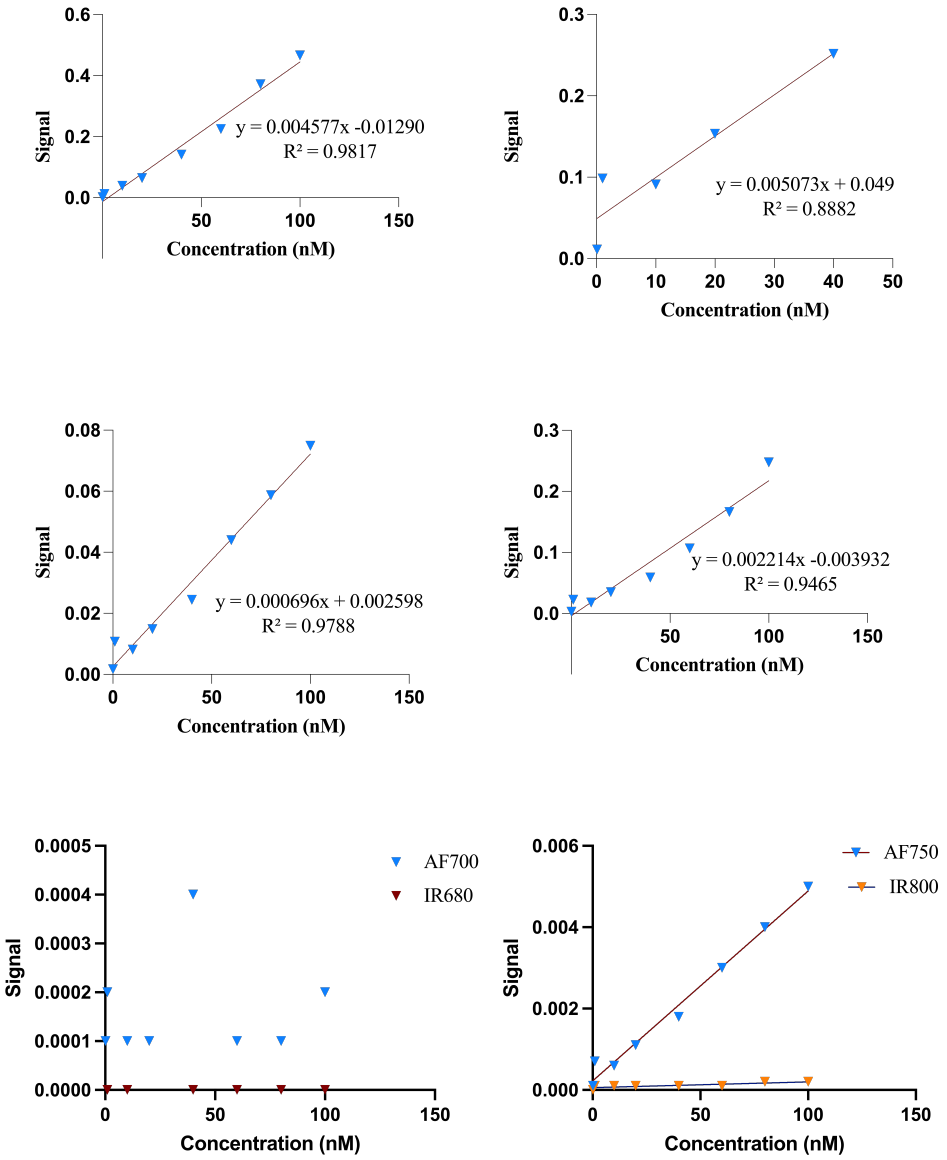

Figure 5. Linearity of signal intensity as a function of dye concentration in the 700 nm and 800 nm detection channels. (a-d) Calibration curves demonstrate linear relationships between dye concentration and signal intensity for each fluorophore in its primary detection channel: (a) IR680 and (b) AF700 in the 700 nm channel; (c) AF750 and (d) IR800 in the 800 nm channel. (e-f) Signal contribution from dyes in their non-primary detection channels (i.e., bleed-through): (e) IR680 and AF700 in the 800 nm channel; (f) AF750 and IR800 in the 700 nm channel.

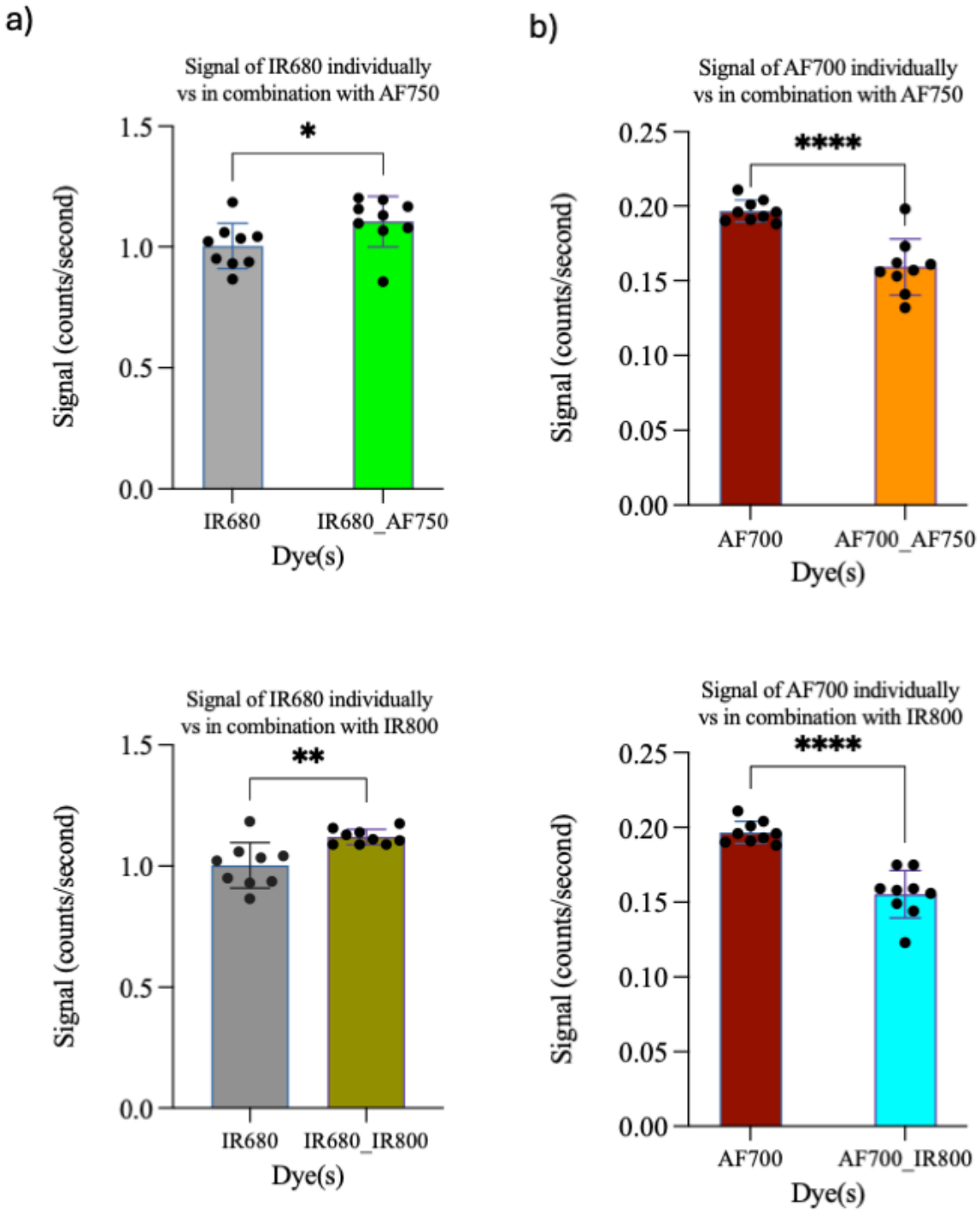

Figure 6. Fluorescence signal intensity comparisons in the 700 nm channel for individual dyes and binary combinations. (a) Signal intensity of IR680 alone vs. in combination with AF750 (top) and IR800 (bottom). (b) Signal intensity of AF700 alone vs. in combination with AF750 (top) and IR800 (bottom). Compared to AF700, IR680 showed minimal signal change when combined with AF750 or IR800, indicating lower spectral cross-talk.

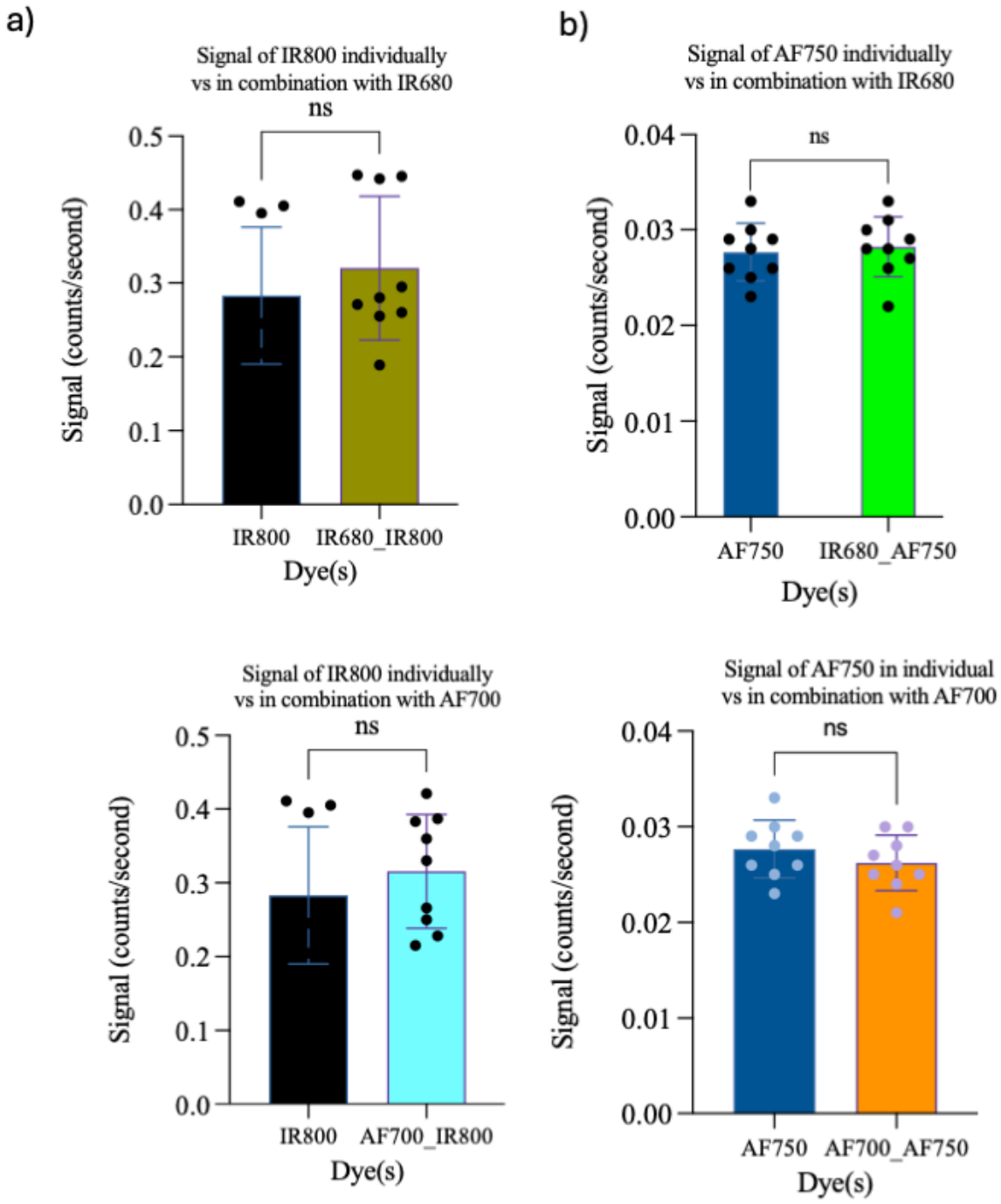

Figure 7. Fluorescence signal intensity comparisons in the 800 nm channel for individual dyes and binary combinations. (a) Signal intensity of AF750 alone vs. in combination with IR680 (top) and AF700 (bottom). (b) Signal intensity of IR800 alone vs. in combination with IR680 (top) and AF700 (bottom). No significant changes in signal were observed, indicating minimal spectral interference in the 800 nm channel.

Chapter 4: Paired Agent Imaging with Soluble PD1

4.1 Introduction

After the quantification of total PDL1 expression on lymphoma tumor cells using mPAI, the next objective was to determine the fraction of PDL1 available for binding to PD1. PDL1 does not only interact in *trans* with PD1 but can also form *cis*-dimers with CD80 on the same cell surface [5]. This cis-interaction sequesters PDL1 and renders it functionally unavailable for PD1 binding. To quantify the available PDL1, that is, the fraction capable of binding PD1, we employed a PAI approach. In this experiment, the targeted agent consisted of a fluorescently labeled soluble PD1 protein, while the untargeted agent was a spectrally distinct free dye.

As with the mPAI experiments, accurate quantification depends on the careful selection of dyes with compatible optical and detection properties. To this end, preliminary liquid phantom experiments were conducted to identify two fluorophores suitable for simultaneous imaging. Linearity assessments were performed to determine the concentration ranges over which each dye exhibited a linear fluorescence response. Subsequently, combination experiments of dyes were conducted to evaluate spectral cross-talk between the 700 nm and 800 nm imaging channels. The combination experiments enabled the selection of dye pairs that could be imaged concurrently without compromising signal specificity.

After the selection of suitable dye pairs, the next step involved determining optimal incubation times for these selected pairs with their respective conjugated proteins. To achieve this, we conducted diffusion experiments utilizing tissue-mimicking phantoms without cells for both the

targeted and untargeted agents. This was followed by tissue-mimicking phantom experiments with lymphoma cells. To quantify the available PDL1 receptors for PD1 binding, a binding potential analysis was performed.

Bibliography

[1] Topalian, S. L., Drake, C. G., and Pardoll, D. M. "Immune Checkpoint Blockade: A Common Denominator Approach to Cancer Therapy". In: *Cancer Cell* 27.4 (2015), pp. 450–461. doi: 10.1016/j.ccell.2015.03.001.

[2] Haslam, A., Gill, J., and Prasad, V. "Estimation of the Percentage of US Patients With Cancer Who Are Eligible for Immune Checkpoint Inhibitor Drugs". In: *JAMA Network Open* 3 (2020), e200423. doi: 10.1001/jamanetworkopen.2020.0423.

[3] Galon, J. and Bruni, D. "Approaches to Treat Immune Hot, Altered and Cold Tumours with Combination Immunotherapies". In: *Nature Reviews Drug Discovery* 18 (2019), pp. 197–218. doi: 10.1038/s41573-018-0007-y.

[4] Ribas, A. and Hu-Lieskovan, S. "What Does PD-L1 Positive or Negative Mean?" In: *The Journal of Experimental Medicine* 213.13 (2016), pp. 2835–2840. doi: 10.1084/jem.20161462.

[5] Sugiura, D., Maruhashi, T., Okazaki, I. M., Shimizu, K., Maeda, T. K., Takemoto, T., and Okazaki, T. "Restriction of PD-1 Function by Cis-PD-L1/CD80 Interactions Is Required for Optimal T Cell Responses". In: *Science* 364.6440 (2019), pp. 558–566. doi: 10.1126/science.aav7062.